Talanta 143 (2015) 178–183

Contents lists available at ScienceDirect

Talanta

journal homepage: www.elsevier.com/locate/talanta

A wireless potentiostat for mobile chemical sensing and biosensing

Matthew D. Steinberg [a], Petar Kassal [b], Irena Kereković [b], Ivana Murković Steinberg [b,*]

[a] GoSense Wireless Ltd., 57A Moorfield Road, Duxford, Cambridge CB22 4PP, UK
[b] Faculty of Chemical Engineering & Technology, University of Zagreb, Marulićev trg 19, HR-10000 Zagreb, Croatia

ARTICLE INFO

Article history:
Received 24 February 2015
Received in revised form
5 May 2015
Accepted 12 May 2015
Available online 22 May 2015

Keywords:
Potentiostat
Amperometry
Biosensor
Glucose test-strip
Radio-frequency identification
Near-field communication
Wireless sensor
Internet of things.

ABSTRACT

Wireless chemical sensors are used as analytical devices in homeland defence, home-based healthcare, food logistics and more generally for the Sensor Internet of Things (SIoT). Presented here is a battery-powered and highly portable credit-card size potentiostat that is suitable for performing mobile and wearable amperometric electrochemical measurements with seamless wireless data transfer to mobile computing devices. The mobile electrochemical analytical system has been evaluated in the laboratory with a model redox system – the reduction of hexacyanoferrate(III) – and also with commercially available enzymatic blood-glucose test-strips. The potentiostat communicates wirelessly with mobile devices such as tablets or Smartphones by near-field communication (NFC) or with personal computers by radio-frequency identification (RFID), and thus provides a solution to the 'missing link' in connectivity that often exists between low-cost mobile and wearable chemical sensors and ubiquitous mobile computing products. The mobile potentiostat has been evaluated in the laboratory with a set of proof-of-concept experiments, and its analytical performance compared with a commercial laboratory potentiostat (R^2=0.9999). These first experimental results demonstrate the functionality of the wireless potentiostat and suggest that the device could be suitable for wearable and point-of-sample analytical measurements. We conclude that the wireless potentiostat could contribute significantly to the advancement of mobile chemical sensor research and adoption, in particular for wearable sensors in healthcare and sport physiology, for wound monitoring and in mobile point-of-sample diagnostics as well as more generally as a part of the Sensor Internet of Things.

1. Introduction

Wireless chemical sensors (WCSs) are analytical devices that combine chemical sensing ability with integrated wireless data transfer. They are particularly suited to mobile and wearable applications where size, weight, power consumption, battery lifetime and connectivity are key factors beyond pure analytical performance. These multiple factors especially come into play where chemical or biological analytes are monitored directly on the body with wearable devices [1], or are measured in-situ in the field [2] or at the point-of-sample with mobile devices [3]. Thanks to the many practical advantages gained from ease-of-use, wide-area coverage, and mobility; specialist wireless chemical sensors are being developed for wearable diagnostics [4], homeland defence [5], environmental monitoring [6], food quality [7] and agriculture [8]. The deployment of mobile WCS systems forms a part of the wider trend in *vanguard–rearguard* analytical strategies [9].

Our research group is developing wireless chemical sensors and systems for mobile and wearable applications based on the near-field communication (NFC) standard [10]. The platform has inputs compatible with the most common (bio)chemical sensors, including optical, conductometric and electrochemical sensors. The novelty of these devices is their intrinsic small size, low-cost, portability and the ability to seamlessly communicate by NFC or radio-frequency identification (RFID) with standard mobile computing devices such as Smartphones, tablets and personal computers, Fig. 1. The value of this approach is that the ubiquitous phone, tablet or computer becomes the instrument, providing computational power, a user interface, a display and higher-level connectivity (Bluetooth, Wi-Fi, and GSM). And in turn, the wireless chemical sensor node which is worn on the body, carried in a pocket, or deployed in a room or in a field remains small, lightweight, mobile, low-cost, highly energy efficient, but yet autonomous and networkable. Integration of an NFC interface into the chemical sensor thus provides low-cost seamless connectivity for the WCS to readily available digital mobile computing products. The specific advantages of RFID/NFC as a communications technology for mobile sensing have been described in detail elsewhere [10,11].

Abbreviations: RFID, radio-frequency identification; NFC, near-field communication; WSN, wireless sensor network; IoT, internet of things

* Corresponding author. Tel.: +385 1 4597 287; fax: +385 1 4829 064.
E-mail address: imurkov@fkit.hr (I.M. Steinberg).

http://dx.doi.org/10.1016/j.talanta.2015.05.028
0039-9140/

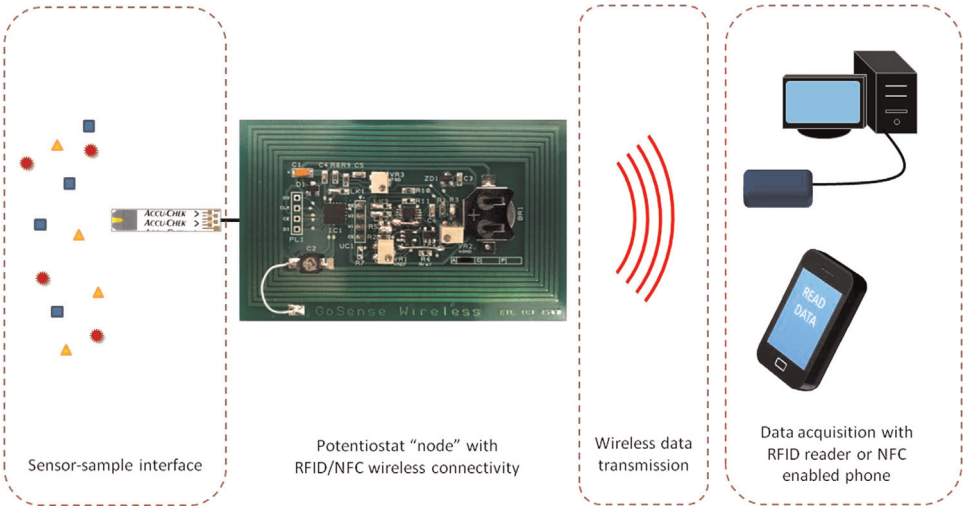

Fig. 1. The wireless potentiostat system illustrated with a glucose test-strip (biosensor) as an exemplary sensor. The biosensor electrodes are conditioned by the potentiostat and the electrochemical current signal is autonomously sampled, digitised and logged to memory, facilitating mobile measurements. Digital data is transferred wirelessly by near-field communication (NFC) to mobile computing devices (Smartphone and tablet) or by radio-frequency identification (RFID) to a personal computer for off-line analysis.

We have previously reported on NFC/RFID-enabled electrochemical devices for ethanol vapour sensing [12], for pH and cations [6,13], and most recently a smart bandage for wound status monitoring [14]. The platform has also been used with optical chemical sensors for pH [15] and potassium ion [16]. Here we present a mobile potentiostat for amperometric electrochemical sensors. Wearable and mobile electrochemical sensors are in development by various research groups [1,2,17,18], and of the common electrochemical measurement techniques available for reading such sensors, chronoamperometry (current–time measurement) is a convenient and widely used methodology that the new potentiostat supports. For healthcare, personal well-being and sport physiology applications, non-invasive biofluids such as saliva, sweat or tears that contain electroactive species are all viable matrices for the system, and potential substrates might include lactate, oxygen, glucose, norepinephrine, nicotinamide adenine dinucleotide (NAD) and hydrogen peroxide [18]. Lactate has been measured by chronoamperometric methods with enzyme modified electrodes in most of the easily available (i.e. non-invasively acquired) biofluids [19–21]. Moreover, wearable sensors have multiple uses beyond ambulatory biometrics and diagnostics, in particular, for monitoring the ambient microenvironment of the user [22]. An interesting example of ambient environment sensing was recently demonstrated with a wearable enzyme electrode for scuba divers [23]. This miniature chronoamperometric system indicates when the concentration of toxic phenolics in the surrounding seawater has exceeded a threshold by illuminating an indicator worn on the diver's neoprene suit.

The wireless potentiostat presented here facilitates the contactless connection of low-cost amperometric electrochemical sensors to ubiquitous mobile computing devices. The potentiostat has been designed, built and subsequently evaluated in the laboratory with proof-of-concept chronoamperometric experiments, initially with potassium ferricyanide in solution as a model redox system and latterly in a series of tests with commercial blood-glucose test-strips. The analytical performance of the system has been compared side-by-side with a laboratory potentiostat.

2. Materials and methods

2.1. Potentiostat with RFID/NFC interface – design

The electronic circuits of the potentiostat and its RFID/NFC interface were designed to fit on a credit-card sized circuit board ($8 \times 5 \times 1$ cm^3) using computer-aided schematic capture and printed circuit board design tools (EASY-PC Professional v13, Number One Systems Ltd., UK). Printed circuit boards were fabricated from standard FR4 materials and populated with surface mount components (RAK Printed Circuits Ltd., UK). The potentiostat nodes communicate wirelessly with a commercially available PC-based RFID reader connected to a USB serial port (HF Development Kit, IDS-Microchip AG, Switzerland). The reader is supplied with software that allows easy set-up of the nodes prior to each experiment (e.g. to set the sample acquisition rate) and to request and manage the transfer of data from a node to the computer after each experiment. Details of the node circuit design are as follows. A low-power analogue potentiostat was designed from micropower integrated circuit amplifiers (OPA336 and INA333, Texas Instruments Inc., Dallas, TX) in a classic transimpedance amplifier configuration [24]. The potentiostat allows connection of two working electrodes in a differential configuration and also connects to a reference and counter electrode, so supports 2-, 3- or 4-electrode cell configurations. The working electrodes' potential is set with respect to the reference electrode with a variable resistor, and can be set over a range from -325 to $+900$ mV. The transimpedance of the INA333 amplifier is 50 kΩ so that the analogue output voltage of the potentiostat, V_{out}, is given by the expression $V_{out}=(i_{wrk1}-i_{wrk2})\times 50$ kΩ where i_{wrk1} is the current measured at the primary working electrode and i_{wrk2} is the current measured at the secondary working electrode. The analogue output voltage, V_{out}, is converted to a digital word by a 10-bit analogue-to-digital converter contained within the RFID/NFC microchip. The wireless interface of the node was designed around an RFID transponder microchip (SL13A, IDS-Microchip AG, Switzerland, since acquired by ams AG, Austria). The interface operates at 13.56 MHz in the high-frequency radio band, and is compliant with the ISO15693 radio-frequency identification (RFID) standard. It is also compatible with Android near-field communication (the NFCv standard). The transponder microchip contains a 10-bit analogue to digital converter (ADC), to

which the analogue output of the potentiostat, V_{out}, was connected. This allows the difference current signal to be digitised at a pre-determined sampling rate, and the resulting digital current–time data stored to memory. Each sample acquisition with the ADC takes approximately 5 ms, and the sample interval can be programmed with the PC software to occur at intervals from 1 sample/s to one sample in 32,768 s. In all experiments, current–time data was measured, digitised and logged autonomously by the mobile potentiostat and then transmitted wirelessly by RFID to a personal computer for off-line analysis in MS-Excel.

2.2. Experimental

All reduction experiments with hexacyanoferrate(III) $[Fe(CN)_6]^{3-}$ (104973, Merck Millipore, Germany) were conducted in a conventional three electrode cell. A gold disc electrode (Au, diameter 1 mm) was used as working electrode and platinum wire and Ag/AgCl electrodes were used as counter and reference electrodes respectively. The Au electrode was polished with Al_2O_3 powder with different particle sizes (1 and 0.25 μm). Subsequent to the mechanical polishing, the electrode was chemically cleaned by immersion in Piranha solution for 5 min ($V(H_2O_2$, 30%):$V(H_2SO_4$, conc.)=1:3; hydrogen peroxide and sulphuric acid were from Kemika, Croatia) and electrochemically in 0.1 M $HClO_4$ (109605, Merck Millipore, Germany) between 0 and 1.5 V vs. the reference electrode until a stable voltammogram was obtained. All chemicals were of analytical grade and all solutions were prepared with deionised water (Milli-Q water purification system, Merck Millipore, USA). The experiments were performed at room temperature after the initial solutions had been deaerated with nitrogen gas for 10 min. The electrodes were connected to the node with crocodile clip connectors. After each experiment the recorded data was wirelessly transferred to a PC for analysis in MS-Excel. All experiments performed with the node were repeated independently on a laboratory potentiostat (Model 264A, Princeton Applied Research, USA) connected to a computer running commercial electrochemical software (EG&G PowerSuite) sampling at a rate of 10 samples/s. The latter system provided reference measurements for correlation with experimental data acquired by the node.

2.2.1. Hydrodynamic reduction of $[Fe(CN)_6]^{3-}$

The node was set to record one sample every 3.5 s, and a reduction potential of −100 mV vs. the reference electrode was applied to the working electrodes. Ten mL of the supporting electrolyte (0.01 M KCl, Kemika, Croatia) was placed in a glass electrochemical cell and the solution continuously stirred by magnetic stirrer. Five successive 100 μL aliquots of 10 mM $[Fe(CN)_6]^{3-}$ were added at 5 min intervals, and the resulting I–t response at the primary working electrode logged by the node. The experiment was independently repeated on a laboratory potentiostat. All experimental raw data was smoothed in MS-Excel with an unweighted moving average (least squares) low-pass filter with a 70 s data window (corresponding to 20 data points for the node and 700 data points for the laboratory potentiostat) [25]. The final current for each concentration of hexacyanoferrate(III) was calculated from the mean of the recorded data between t=230 and 300 s after addition of each aliquot. The experiment was repeated two further times, and a mean current determined for each concentration of $[Fe(CN)_6]^{3-}$.

2.2.2. Diffusion controlled reduction of $[Fe(CN)_6]^{3-}$

Diffusion controlled measurements were performed by programming the node to record one sample every 1.2 s and setting a reduction potential at the working electrodes of −100 mV vs. the reference electrode. The electrodes were then disconnected from the node. A 100 μL addition of 10 mM $[Fe(CN)_6]^{3-}$ was added to 10 mL of the supporting electrolyte (0.01 M KCl). After the addition, the solution was stirred for 1 min followed by 15 s of (unstirred) equilibration time. At this point the node was connected to the electrodes and allowed to log data for 3 min, after which the recorded data was wirelessly transferred to the PC. The first 70 s of data from the 3 min recording was plotted in MS-Excel. The same procedure was then repeated for four more sequential additions of 100 μL of 10 mM $[Fe(CN)_6]^{3-}$. The experiment was independently repeated on a laboratory potentiostat.

2.2.3. Glucose determination

Accu-Chek® Performa glucose test-strips (06454011, Roche Diagnostics GmbH, Germany) were obtained from a local dispensing pharmacy in boxed lots of 50 pieces. During experiments individual test-strips were connected to the node with micro-clip connectors, with the counter and reference electrode connections of the node short-circuited together. The voltage between the working and counter/reference electrodes was set to +300 mV. A 0.1 M phosphate buffer solution (pH=7.39) was prepared by dissolving disodium hydrogen phosphate dihydrate and sodium dihydrogen phosphate dihydrate (Kemika, Croatia) in deionised water. Buffered glucose solutions (c=0.1, 0.3, 1, 2, 3, 4, 6, 8 and 10 mM) were prepared by dissolving D-(+) glucose (47829, Sigma-Aldrich, USA) in the phosphate buffer solution. The experimental protocol was as follows: the amperometric node (connected to a glucose test-strip) was set to record one sample every 1.2 s. After 1 min of logging to acquire a baseline, the sample inlet port of the test-strip was lightly touched to a 5 μL droplet of buffered glucose solution which had previously been dispensed by pipette on to a hydrophobic (glass) surface. After allowing the glucose solution to wick into the test-strip by capillary action, the test-strip was placed horizontally on the bench and the node was allowed to log data for an additional 3 min, after which time the recorded data was transferred wirelessly to a PC for analysis.

3. Results and discussion

3.1. Potentiostat with RFID/NFC interface – performance

Our approach to the development of wireless chemical sensor nodes is to endow the chemical sensor with a low-cost seamless digital interface that is machine readable. This strategy is designed to enable inexpensive mobile WCSs to connect with ubiquitous consumer products such as Smartphones, tablets and computers. In this work, a battery powered WCS potentiostat has been successfully developed with an RFID/NFC wireless interface. The RFID/NFC standard was developed for the purpose of connecting simple, low-cost, low data-rate devices (ID tags, smartcards, contactless credit cards etc.) to electronic networks. Unlike other short-range wireless standards often used for WCSs such as Wi-Fi, Bluetooth [8,22] and ZigBee, NFC can be implemented in the simple device without need for a microprocessor, memory, a radio transmitter or battery [10]. This keeps the cost, complexity, size and power consumption of the WCS to a minimum. The potentiostat is the size of a thick credit card ($80 \times 50 \times 10$ mm^3) so is highly portable but also wearable and fits easily into a pocket or ID badge holster. It has connections on the input side suited to amperometric biosensors or to the electrodes of any electrochemical cell as demonstrated in this work. The node was found to accurately measure, convert and store amperometric (current) signals as digital words with a linear calibration relationship $D_{word}=0.0871i+551.18$ ($R^2=1$) where D_{word} is the stored digital value and $i=i_{wrk1}-i_{wrk2}$. Digital data was transferred to a personal computer by RFID for analysis. In laboratory conditions at room temperature

the mobile potentiostat operated from a 3 V lithium coin cell with a quiescent current of less than 100 μA, rising to 200 μA during a sample acquisition that takes 5 ms to complete. Transmission of data to a PC by RFID or a Smartphone by NFC does not consume any additional battery power since data is sent by passive near-field modulation of the receiving device's 13.56 MHz carrier wave. The input range of the potentiostat was determined as ±5400 nA and found to be linear over measured current values from 15 to 4394 nA. The least significant bit of the ADC which is equivalent to the maximum achievable resolution was found to be 11.5 nA, and the limit of detection (LOD) of the potentiostat was ±15 nA. The potentiostat was able to perform chronoamperometric reduction and oxidation experiments with excellent correlation to a laboratory potentiostat (R^2=0.9999) as demonstrated below.

3.2. Hydrodynamic reduction of $[Fe(CN)_6]^{3-}$

The well known redox system $[Fe(CN)_6]^{3-} + e^- \rightarrow [Fe(CN)_6]^{4-}$ was used to characterise the chronoamperometric function of the node in hydrodynamic controlled experiments [26]. Different concentrations of hexacyanoferrate(III) in solution were measured in the range from 100 to 500 μM in stirred buffers in a 3-electrode cell. Chronoamperograms (current–time response) were measured with a laboratory potentiostat (A) and with the wireless potentiostat node (B), Fig. 2. Each step corresponds to an addition of 100 μL of 10 mM $[Fe(CN)_6]^{3-}$. The plot of final mean reduction current against $[Fe(CN)_6]^{3-}$ concentration was found to be linear as expected for this concentration range (i=0.0033c+0.1334, R^2=0.999, where i=reduction current in μA and c=concentration of hexacyanoferrate(III) anion in μM), Fig. 2 inset. Experimental repeatability was calculated from the standard deviation of the data as indicated by error bars, and was found to be better than 5%. Correlation with the laboratory potentiostat showed excellent agreement between the two instruments (y=0.9155x+0.0084, R^2=0.9999).

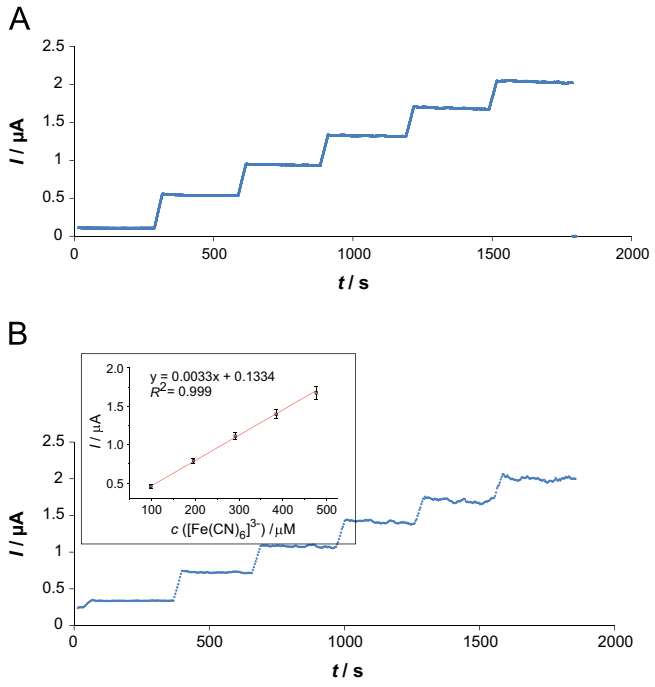

Fig. 2. Chronoamperograms (current–time response) measured with a laboratory potentiostat (A) and with the wireless potentiostat node (B) during the hydrodynamic reduction of hexacyanoferrate(III) anion. Each step corresponds to an addition of 100 μL of 10 mM $[Fe(CN)_6]^{3-}$. Inset: correlation of the final mean reduction current measured with the wireless potentiostat as a function of $[Fe(CN)_6]^{3-}$ concentration (n=3, mean ± S.D.).

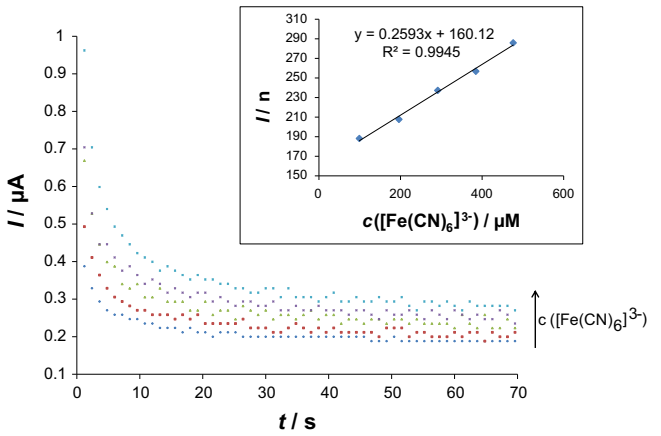

Fig. 3. Chronoamperograms (current–time response) measured with the wireless potentiostat during diffusion controlled reduction of hexacyanoferrate(III) anion. Each curve represents the addition of 100 μL of 10 mM $[Fe(CN)_6]^{3-}$ (increasing current). Inset: calibration function for mean final current vs. $[Fe(CN)_6]^{3-}$ concentration.

3.3. Diffusion controlled reduction of $[Fe(CN)_6]^{3-}$

Chronoamperograms obtained for the diffusion controlled reduction of $[Fe(CN)_6]^{3-}$ are shown, Fig. 3. Cottrell equations to describe the transient current response from the experimental data could not be determined with high accuracy because of the limited sample acquisition rate of the potentiostat node (1 sample every 1.2 s). It was however observed that the current equilibrates after a set time period, and the final steady state current could be used as the analytical parameter. The final current was therefore computed as the mean of 20 data points around t=60 s. The relationship between the final steady state current and the $[Fe(CN)_6]^{3-}$ concentration was found to be linear, Fig. 3 inset.

3.4. Glucose sensing experiments

After demonstrating the functionality of the amperometric node in diffusion controlled experiments, its performance was evaluated with glucose test-strips. The test-strips are commercially available enzymatic biosensors in which the electrochemical reaction is also diffusion controlled. The strips were connected to the potentiostat node in a 2-electrode configuration (working-electrode with a common counter/reference electrode) and used to determine glucose concentration in physiological buffers over a range of 0.1–10 mM glucose. Because commercial glucose test-strips are produced in large batches with close manufacturing tolerances they have good intra-batch reproducibility. The Accu-Chek® Performa strips work by catalysing the oxidation of D-glucose to D-glucono-1,5-lactone in the presence of the co-enzyme pyrroloquinoline, which is simultaneously reduced [27]. The chronoamperometric response of different test-strips connected to the node upon exposure to buffered glucose solutions was determined, Fig. 4. Similar to the diffusion controlled reduction of $[Fe(CN)_6]^{3-}$, the final steady state current was taken as the analytical parameter measured at a set time after applying the glucose solution to the test-strip. The final current was calculated as the mean of 20 data points recorded between t=156 s and t=180 s after wicking of the glucose solution. The experiment was repeated six times (with 6 different test-strips) for each glucose concentration to generate a calibration curve, Fig. 4 inset. Regression analysis confirmed the data to be linear, and the best line fit was thereafter used as a multi-point calibration function for the batch (i=62.155c(glucose)+10.993, R^2=0.9991 where i is the oxidation current in nA and c(glucose) is concentration in mM).

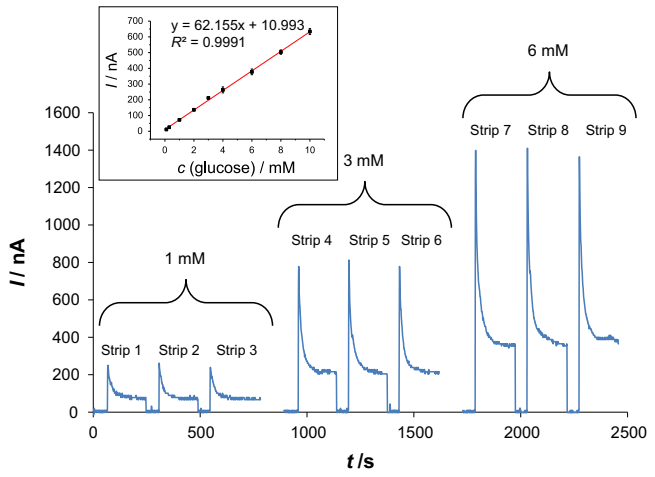

Fig. 4. Chronoamperograms (current–time response) of the wireless potentiostat node connected to glucose test-strips on exposure to glucose standards. Each curve represents a single measurement with a different test-strip as indicated (strips 1, 2, 3 are in 1 mM; strips 4, 5, 6 are in 3 mM; and strips 7, 8, 9 are in 6 mM glucose solution). Inset: calibration function of the wireless potentiostat with commercial glucose test-strips (n=6, mean ± S.D.).

This demonstrates the steady-state linearity of the system over the physiologically relevant range up to 10 mM glucose. The precision of the biosensor measurement system was calculated by one standard deviation from the mean final current, as indicated with error bars, Fig. 4 inset. The standard deviation was less than 19 nA over the measured range, which in terms of glucose concentration, calculated from the batch calibration function, is equivalent to less than 0.3 mM. The limit of detection (LOD) was 0.18 mM glucose calculated using the $\mu+3\sigma$ methodology.

4. Conclusion

A wireless amperometric potentiostat has been presented that offers a solution to the 'missing link' in wireless data connectivity that exists between simple low-cost mobile and wearable chemical sensors and powerful ubiquitous computing products (Smartphones, tablets, and computers). By providing a seamless digital interface, the new potentiostat could assist in the commercial realisation and widespread adoption of wearable and mobile electrochemical sensors. The potentiostat is semi-autonomous and operates as a stand-alone chronoamperometric data logger, with data analysis performed externally on the Smartphone, tablet or computer. The instrumental and analytical performance of the potentiostat has been evaluated in the laboratory and the results confirm the device is suited to mobile, wearable and point-of-sample sensor applications. In addition to a series of classical solution-based reduction experiments, the potentiostat has been shown to function with commercial enzyme-based amperometric biosensors, which is an important step toward the practical realisation of textile wearable sensors [28] and wearable electrochemical sensors in general [1,18,21,23]. We stress that in this work we have not undertaken to address the many complex challenges surrounding wearable sensor design, least of all sample collection, sample delivery (to the sensing surface), and sensor fabrication and durability. We do however present a viable solution for the 'missing link' in connectivity that will allow simple analogue chemical sensors to interface seamlessly with ubiquitous mobile computing products. The system has recently been demonstrated with a smart bandage biosensor for monitoring the status of chronic wounds [14].

We conclude that the wireless potentiostat could contribute significantly to the advancement of mobile chemical sensor research and adoption, in particular for wearable sensors in healthcare and sport physiology, for wound monitoring and in mobile point-of-sample diagnostics [29] as well as more generally as a part of the Sensor Internet of Things.

Acknowledgements

These materials are based on work supported by the University of Zagreb, under research grant number 110011 (2013), 'Integrated analytical chemical systems: development and application of chemical sensors and biosensors.'

References

[1] J.R. Windmiller, J. Wang, Electroanalysis 25 (2013) 29–46.
[2] C. Zuliani, D. Diamond, Electrochim. Acta 84 (2012) 29–34.
[3] A. Nemiroski, D.C. Christodouleas, J.W. Hennek, A.A. Kumar, E.J. Maxwell, M. Teresa Fernandez-Abedul, G.M. Whitesides, Proc. Nat. Acad. Sci. USA 111 (2014) 11984–11989.
[4] T. Guinovart, G. Valdes-Ramirez, J.R. Windmiller, F.J. Andrade, J. Wang, Electroanalysis 26 (2014) 1345–1353.
[5] R.A. Potyrailo, N. Nagraj, C. Surman, H. Boudries, H. Lai, J.M. Slocik, N. Kelley-Loughnane, R.R. Naik, TrAC Trends Anal. Chem. 40 (2012) 133–145.
[6] M. Novell, T. Guinovart, I.M. Steinberg, M. Steinberg, F.X. Rius, F.J. Andrade, Analyst (2013).
[7] R.A. Potyrailo, N. Nagraj, Z.X. Tang, F.J. Mondello, C. Surman, W. Morris, J. Agric. Food Chem. 60 (2012) 8535–8543.
[8] L. Ruiz-Garcia, L. Lunadei, P. Barreiro, J.I. Robla, Sensors 9 (2009) 4728–4750.
[9] M. Valcarcel, S. Cardenas, TrAC Trends Anal. Chem. 24 (2005) 67–74.
[10] E. Strömmer, M. Hillukkala, A. Ylisaukko-oja, Ultra-low power sensors with near field communication for mobile applications, in: L. Orozco-Barbosa, T. Olivares, R. Casado, A. Bermúdez (Eds.), Wireless Sensor and Actor Networks, Springer, US, 2007, pp. 131–142.
[11] L. Atzori, A. Iera, G. Morabito, Comput. Netw. 54 (2010) 2787–2805.
[12] M.D. Steinberg, I. Zura, I.M. Steinberg, Sens. Actuators B: Chem. 196 (2014) 208–214.
[13] P. Kassal, I.M. Steinberg, M.D. Steinberg, Sens. Actuators B: Chem. 184 (2013) 254–259.
[14] P. Kassal, J. Kim, R. Kumar, W.R. de Araujo, I.M. Steinberg, M.D. Steinberg, J. Wang, Electrochem. Commun. 56 (2015) 6–10.
[15] I.M. Steinberg, M.D. Steinberg, Sens. Actuators B: Chem. 138 (2009) 120–125.
[16] M.D. Steinberg, P. Kassal, B. Tkalcec, I.M. Steinberg, Talanta 118 (2014) 375–381.
[17] D. Morris, B. Schazmann, Y. Wu, S. Coyle, S. Brady, C. Fay, J. Hayes, K.T. Lau, G. Wallace, D. Diamond, Conference Proceedings: Annual International Conference of the IEEE Engineering in Medicine and Biology Society, IEEE Engineering in Medicine and Biology Society, 2008, pp. 5741–5744.
[18] A.J. Bandodkar, J. Wang, Trends Biotechnol. 32 (2014) 363–371.
[19] N. Thomas, I. Lähdesmäki, B.A. Parviz, Sens. Actuators B: Chem. 162 (2012) 128–134.
[20] W. Jia, A.J. Bandodkar, G. Valdés-Ramírez, J.R. Windmiller, Z. Yang, J. Ramírez, G. Chan, J. Wang, Anal. Chem. 85 (2013) 6553–6560.
[21] J. Kim, G. Valdes-Ramirez, A.J. Bandodkar, W. Jia, A.G. Martinez, J. Ramirez, P. Mercier, J. Wang, Analyst 139 (2014) 1632–1636.
[22] F. Tsow, E. Forzani, A. Rai, R. Wang, R. Tsui, S. Mastroianni, C. Knobbe, A.J. Gandolfi, N.J. Tao, IEEE Sens. J. 9 (2009) 1734–1740.
[23] K. Malzahn, J.R. Windmiller, G. Valdes-Ramirez, M.J. Schoening, J. Wang, Analyst 136 (2011) 2912–2917.
[24] M.D. Steinberg, C.R. Lowe, Sens. Actuators B: Chem. 97 (2004) 284–289.
[25] A. Savitzky, M.J.E. Golay, Anal. Chem. 36 (1964) 1627–1639.
[26] G.I.H. Hanania, D.H. Irvine, W.A. Eaton, P. George, J. Phys. Chem. 71 (1967) 2022–2030.
[27] Anon, Evaluation Report: ACCU-CHEK® Aviva System, Roche Diagnostics, 2007.
[28] M.-C. Chuang, J.R. Windmiller, P. Santhosh, G.V. Ramirez, M. Galik, T.-Y. Chou, J. Wang, Electroanalysis 22 (2010) 2511–2518.
[29] E. Ghafar-Zadeh, Sensors 15 (2015) 3236–3261.

Matthew D. Steinberg is a co-founder and director of GoSense Wireless Ltd. He holds a B.Eng. degree in Electronic Engineering from the University of Liverpool,

and a Ph.D. from the Institute of Biotechnology, University of Cambridge. His research interests are in healthcare diagnostics and microsystems technology, particularly the integration of sensors and low-power communications for mobile health monitoring.

Petar Kassal is a Teaching Assistant at the Faculty of Chemical Engineering & Technology, University of Zagreb, Croatia, where he is currently working towards a Ph.D. He received his B.Eng. degree in Chemical Engineering from the same faculty in 2010. His doctoral research is the development and integration of optical and electronic devices into wireless chemical sensors.

Irena Kereković is a postdoctoral Research Assistant at the Faculty of Chemical Engineering & Technology, University of Zagreb, Croatia. Irena received her Ph.D. in chemistry in 2011. Her research interest is the design of sensor interfaces for detection of diverse analytes, predominantly targeting human applications.

Ivana Murković Steinberg is an Assistant Professor at the Faculty of Chemical Engineering & Technology, University of Zagreb, Croatia. She graduated with a B.Eng. degree in Chemical Engineering from that faculty, and obtained a Ph.D. from the University of Graz, Austria, in optical chemical sensors. Her current research involves development of novel functional materials and (bio)chemical sensing architectures particularly suited for integration with wireless sensing platforms.